Acceleration Trajectory Analysis in Remote Gait Monitoring*

Pawel Badura[1] and Ewa Pietka[1], *Member, IEEE* and Stanislaw Franiel[1]

***Abstract*— The study demonstrates part of an ambient assisted living system developed for the remote care of the elderly. Described methods and experiments involve acceleration-based trajectories analysis that yields a feature vector to be subjected to an expert system able to create an individual patient's model by learning high-level features of her/his motion. At this stage we have implemented a footstep detector that permits each foot movement to be analyzed separately and described in terms of predefined features. By mounting the sensors at five various locations on the subjects body, we have indicated areas that feature a high sensitivity to the measurement of abnormal step incidents. Our experiments demonstrate also features able to distinguish abnormal patient motion.**

I. INTRODUCTION

Aging of contemporary societies makes well-being and safety of the elderly one of the major concerns in health care. Since the continuous support (*e.g.* in hospitals or assisted living facilities) is necessary in the minority of cases, remote systems for home supervision and assistance become more important and popular nowadays. Monitoring, processing and transmission resources provided for alert generation in threats might be employed and broaden to offer more sophisticated tools for identification of selected individual patient's features. That leads to the creation of some sort of a subject-specific model on the basis of one's standard behaviour (overall and detailed motion characteristics, activity time distribution etc.) With such a model, each short- and long-term disturbances might be detected and cause an appropriate reaction. A broad review of such Ambient Assisted Living (AAL) systems architecture and abilities have been drawn by Mitas et al. [1]. Although they employ various acquisition techniques and devices, *e.g.* PIR movement detectors [2], cameras [3], radio wave or ultrasound beacons [4], the wearable sensors are more flexible and less demanding in terms of the amount of necessary equipment. The topic of inertial sensors employment for activity monitoring is well known and investigated [5], [6], [7], [8].

The goal of this study is to extract acceleration-based features that indicate significant changes of patient walk steps that might cause a threat of the fall or even an actual fall. Thus, two phases are distinguished. First, the step detection method is developed, then, the step-gated analysis of the walk trajectory is performed.

The following subsections present the overall ambient assisted living system and the mobile data acquisition device. Section II describes the input data, their preprocessing, step detection, walk trajectories, and features extracted for each walk step. Section III presents the experimental results. Section IV concludes the presentation.

A. AMBIENT ASSISTED LIVING SYSTEM

The AAL system described in this paper is developed to meet certain requirements, i.e. (1) to be able to detect possible incidents and threats, causing an immediate remote reaction, (2) to estimate patient's individual characteristics in terms of motion (gait) features, and then to reliably supervise and predict short-term risk of dangerous situations, (3) to provide comprehensive information about the changes in patient's health and life quality via long-term monitoring, and (4) to acquire data from various sources (*e.g.* sensors and interactive devices to allow patient's conscious interference). All necessary devices should not disturb or even be unnoticeable for the patient.

The basic element of the system [9], i.e. the mobile data acquisition device (MDAD) collects the data from various sensors worn by the patient, preprocesses and forwards it to the home endpoint (HE). HE transmits the data to the central system, which stores, analyses and monitors the data.

B. MOBILE DATA ACQUISITION DEVICE

The MDAD is supposed to collect the data and isolate the diagnostically important information about the patient's activity. MDAD receives signals from inertial sensors, distributed over a patient's body, each containing 3-axial accelerometer and gyroscope (MPU6050 modules).

Those data might be treated in miscellaneous forms, according to the AAL system fundamentals [9]. On one hand, a detection of incidents and threats initiates immediate reaction; on the other hand, the variability of patient's behavior is acquired. The latter refers to all unexpected and potentially dangerous patterns in the patient's activities, including also long-term changes in the motion features, as possible indicators of abnormal symptoms.

Our concern in this study is to analyze possible number and distribution of sensors in terms of their sensitivity in the monitoring system. Several aspects have to be taken into consideration and balanced:

- contribution brought by kinetic information from various body parts,
- ergonomics in terms of wearing simplicity and comfort (*e.g.*, as a part of clothes, belt, watch, etc.),
- data redundancy, constrained by the system transmition, storage and processing abilities.

*This work has been supported by the European Union under the 7th Frame Programme grant nr POIG.01.03.01-24-061/12.

[1]P. Badura, E. Pietka and S. Franiel are with Faculty of Biomedical Engineering, Silesian University of Technology, 41-800 Zabrze, Poland `pawel.badura at polsl.pl, ewa.pietka at polsl.pl`

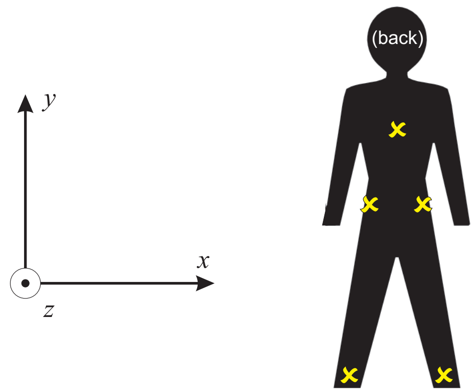

(a) (b)

Fig. 1. Inertial sensor orientation (a) and locations during experiments (b)

To do so, we investigate acceleration and velocity information from inertial sensors in terms of their real-time trajectory plots, employing a step detection and description algorithm. We also propose distinctive features in order to indicate specific motion properties.

II. MATERIALS AND METHODS

A. Input Data

Since in this study we focus on a human walk monitoring, we use only inertial sensors as input data sources. Fig. 1a shows the space orientation, that has been defined for each sensor with respect to the patient. We have tested various sensor locations (Fig. 1b): back (at T6 vertebra), hips and ankles. Correlation analysis for the MDAD with five sensors placed on the patient's back has been discussed in the previous work [9].

With sampling frequency f_s set to 100Hz, each sensor produces two 3-element samples:

- acceleration $\mathbf{a}(t) = [a_x(t), a_y(t), a_z(t)]^T$ normalized with respect to the gravitational acceleration g,
- angular velocity $\omega(t) = [\omega_x(t), \omega_y(t), \omega_z(t)]^T$ in radians per second.

B. Data Preprocessing

Multiple procedures have been tested and appended into the acceleration signal preprocessing workflow. That includes both, low-pass (median with window size at 15) and high-pass filtering (elliptic IIR with cutoff frequency at 0.2Hz), in order to eliminate high frequency noise and directional acceleration offset, respectively. We have also employed an algorithm for the offset detection and subtraction to avoid nonlinear phase distortions brought by the IIR filter in a ca.-1Hz range. Note, that both high-pass filters successfully remove g (gravity of Earth) from the a_y component. The gyroscope data have been employed by the quaternion-based algorithm [10], [11] for the virtual sensor rotation to the default position, applied to predict and remove the gravitational acceleration influence on each of the sensor axis.

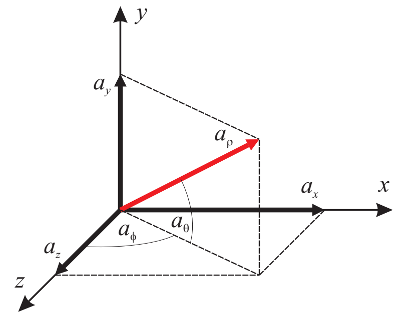

Fig. 2. Acceleration Cartesian vs. spherical coordinate system

Based on the offset-free acceleration vector, a complete set of samples is computed in time t:

- acceleration vector in spherical coordinate system $\mathbf{a}(t) = [a_\rho(t), a_\theta(t), a_\phi(t)]^T$ (Fig. 2), where:

$$\mathbf{a}_\rho(t) = \sqrt{a_x(t)^2 + a_y(t)^2 + a_z(t)^2}, \quad (1)$$

$$\mathbf{a}_\theta(t) = arctan\left(\frac{a_y}{\sqrt{a_x(t)^2 + a_z(t)^2}}\right), \quad (2)$$

$$\mathbf{a}_\phi(t) = arctan\left(\frac{a_x}{a_z}\right), \quad (3)$$

- velocity $\mathbf{v}(t) = [v_x(t), v_y(t), v_z(t)]^T$:

$$\mathbf{v}(t) = \int_0^t \mathbf{a}(\tau)d\tau. \quad (4)$$

C. Step Detection

Reliable step detection is the first stage of the walk features extraction. Since the vertical acceleration indicates mostly the gait peaks, the a_y component is employed to detect the steps. Several constraints have been formulated to reject false positive detections:

- peak shape conditions in terms of a minimum margin of protrusion over surrounding minima and its width in time domain,
- peak-to-peak interval time limits.

All quantitative limitations, initially set to standard values averaged through a large population, are adapted individually during the learning phase.

D. Cartesian and Spherical Step-Gated Trajectories

Patient's walk might be described by a standard step trajectory, acquired during a learning period. All short- and long-term variations are supposed to serve as primary alert sources.

A single step trajectory is determined by a linear interpolation of the acceleration component a_c (with $c = \{x, y, z\}$ or $c = \{\rho, \theta, \phi\}$ in Cartesian and spherical coordinate system, respectively), gated by the current step timestamps. Interpolation secures an equal length of all steps' trajectories, which is necessary to enable a comprehensive inter-step analysis. According to the sampling frequency, average step

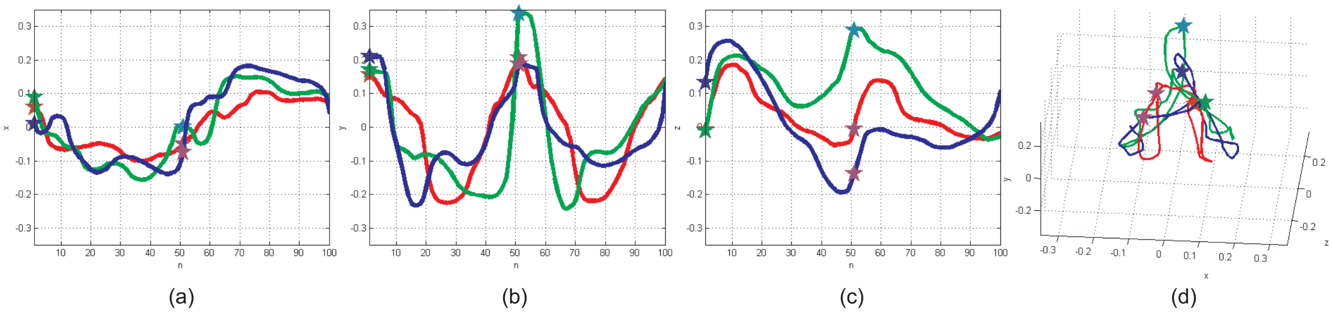

Fig. 3. Step acceleration trajectories for different gait types (single patient each, averaged throughout a $60s$ period): normal walk (red), left leg limp (blue), right leg limp (green). Left to right: a_x, a_y, a_z coordinates as a function of a sample number n (a)-(c), respectively, and a 3D plot of $\mathbf{a}(n)$ (d). A single plot covers two steps (left and right), stars indicate the step beginning. The sensor is located on patient's back (T6 vertebra).

duration and required accuracy level, the number of points per step has been set to $N_{pps} = 50$.

Valuable observations can be done on trajectory plots. Fig. 3 shows sample averaged trajectories of a walk observation for three different types of gait: normal walk, left- and right leg limp. Since the peak detection algorithm (Section II-C) produces subject-invariant reference time sequence of each step, the procedure might be employed to draw velocity trajectories as well.

E. Secondary Features

The step-gated trajectories are subjected to the features extraction phase. In this study two types of features are introduced. The first one is related to the step description, the other reflects the trajectory shape.

The step description features result from the 2D trajectories yielding the step duration, left-to-right step duration ratio, the foot deviation from the waking direction, the full cycle (double) step frequency and a comprehensive step analysis in frequency domain — using the Discrete Fourier Transform (DFT) [12], etc.

The 3D trajectory shape (Fig. 3d) is reflected by the ellipsoid with the same second-order moments as the set of trajectory points in Cartesian coordinate system [13]. Thus, the ellipsoid center, area, major and minor axes lengths with their ratio, the major axis direction, eccentricity are extracted. Fig. 4 shows projections of the ellipsoid onto each of the three planes x-z, x-y and z-y for trajectories from Fig. 3. The ellipsoid-based analysis is also useful in a continuous analysis, i.e. setting a fixed, few-second time window provides a sufficient amount of samples to cover few steps or inactivity moment and deliver necessary data to the inference system.

III. EXPERIMENTAL RESULTS

A. Evaluation of Step Detection

The step detection algorithm has been evaluated using a database of 70 various gait signals obtained during experiments involving 8 patients. Detection has been performed with reference signals taken from different body locations. Table I presents the sensitivity results yielded for three gait modes: normal walk, left and right limp, whilst Table II shows the step side assignment summary (both experiments averaged across different subjects). The back is the most reliable location, with high efficiency in both tasks. Although the ankle locations produce the largest acceleration peaks, their asymmetry makes the leg-dependent observations difficult. Furthermore, any pathological changes of the limbs shortens the acceleration peaks. Thus, the back location proves to be the most promising in step detection during various modes of shuffling, yet due to a small amplitude of the a_y component, the employment of a_x is inevitable.

TABLE I
STEP DETECTION SENSITIVITY

Sensor location	Normal walk	Left leg limp	Right leg limp
Back (T6)	99.30%	99.87%	99.61%
Left hip	89.55%	87.10%	94.59%
Right hip	87.89%	86.29%	97.30%
Left ankle	98.10%	85.48%	99.23%
Right ankle	99.05%	97.58%	72.97%

TABLE II
STEP SIDE ASSIGNMENT SENSITIVITY

Sensor location	Normal walk	Left leg limp	Right leg limp
Back (T6)	99.69%	100.00%	100.00%
Left hip	78.78%	96.76%	91.02%
Right hip	76.76%	70.56%	98.41%
Left ankle	100.00%	99.06%	100.00%
Right ankle	98.56%	100.00%	92.06%

B. Incident Detection Using Ellipsoid-Based Features

An ellipsoid described in Section II-E has been employed to indicate unusual patterns in gait signal. Two particular incidents have been extracted from the standard walk course: sudden leans against the wall and slips. Fig. 5 shows plots of ellipses areas (ellipsoid projection onto Cartesian planes) during the disturbed gait periods (arrows indicate the incidents). The ellipses' areas detect sudden accelerations in given directions, whilst the other features distinguish steps and incidents.

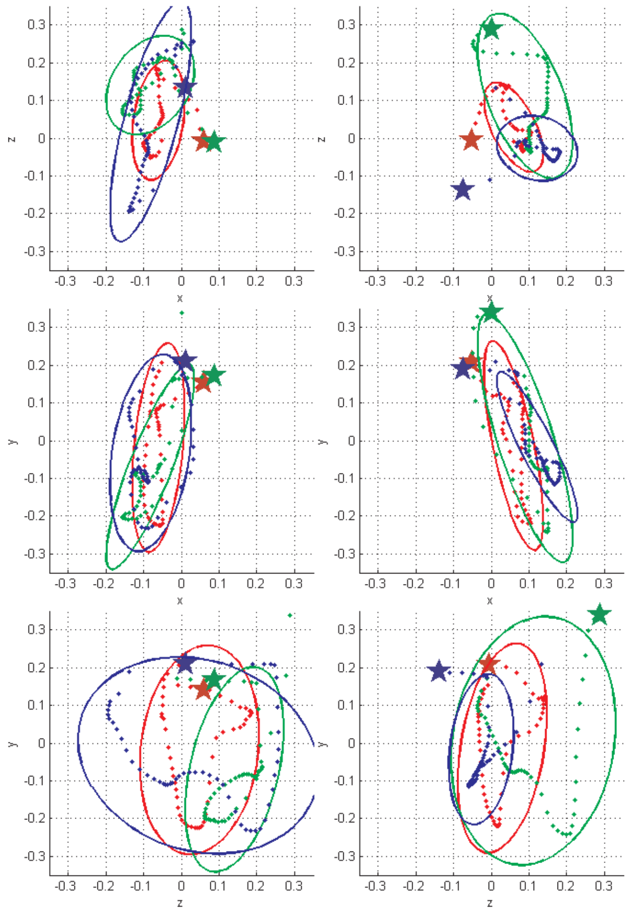

Fig. 4. Ellipsoid projections of trajectories form Fig. 3 onto three basic Cartesian planes: normal walk (red), left leg limp (blue), right leg limp (green). Left column refers to left step, right column — to right step. Stars indicate the step beginning, samples are shown as points.

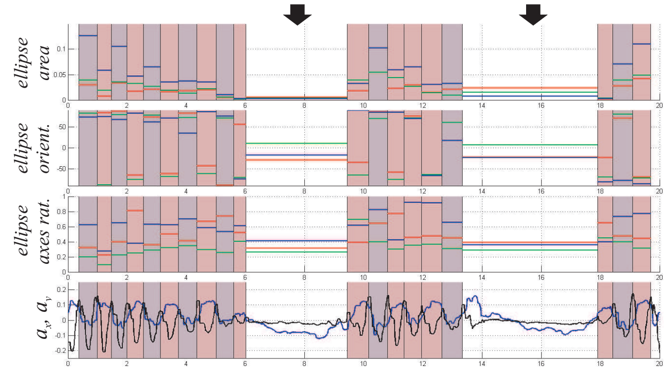

(a)

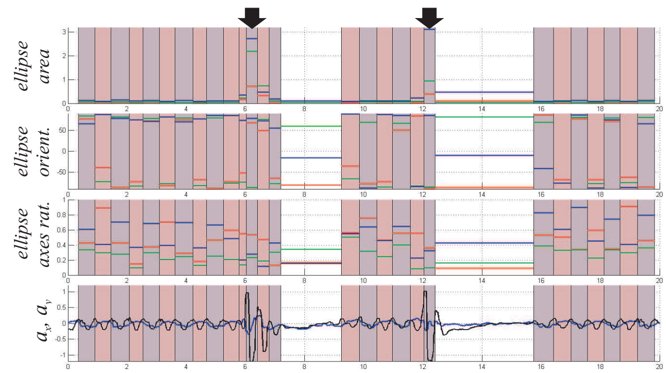

(b)

Fig. 5. Step-gated ellipsoid projections features (area, orientation, minor to major axis ratio) plots during gait: detections (arrows) of sudden left side leans (a) and slips (b). A given ellipse feature value is shown for each detected step: ellipses on the x-z (red), x-y (green), z-y (blue) planes. The lowest chart shows the a_y (black) and $a_x(t)$ (blue) plots. Vertical stripes indicate the detected steps: left(violet and right (pink). The sensor is located on patient's back (T6 vertebra).

IV. CONCLUSIONS

The procedures, features and conclusions presented in this paper stand for the first phase ot the study on an intelligent remote AAL system for the elderly care in home environment. Since the capabilities of motion observation prove to offer comprehensive information about patient's activity, we currently look forward to the employment of a knowledge-based and adaptable expert systems for model creation and automated supervision with reliable reports on patient's conditions.

REFERENCES

[1] A. Mitas, M. Rudzki, M. Skotnicka, P. Lubina, Activity Monitoring of the Elderly for Telecare Systems – Review. In: E. Pietka, J. Kawa, W. Wieclawek (eds.) Information Technologies in Biomedicine, Advances in Intelligent Systems and Computing, Springer-Verlag, (in press).

[2] C. Yang, Y. Hsu, Remote Monitoring and Assessment of Daily Activities in the Home Environment. Journal of Clinical Gerontology and Geriatrics, vol. 3, no. 3, pp. 97–104, 2012.

[3] A. Costa, J. Castillo, P. Novais, A. Fernandez-Caballero, R. Simoes, Sensor-Driven Agenda for Intelligent Home Care of the Elderly. Expert Systems with Applications, vol. 39, no. 15, 12192–12204, 2012.

[4] A. Marco, R. Casas, J. Falco, H. Gracia, J. Artigas, A. Roy: Location-Based Services for Elderly and Disabled People. Computer Communications, vol. 31, no. 6, pp. 1055–1066, 2008.

[5] M. Nyan, F. Tay, K. Seah, Y Sitoh, Classification of Gait Patterns in the TimeFrequency Domain, Journal of Biomechanics, vol. 39, no. 14, pp. 2647–2656, 2006.

[6] A. Godfrey, R. Conway, D. Meagher, G. OLaighin, Direct Measurement of Human Movement by Accelerometry, Medical Engineering & Physics, vol. 30, no. 10, pp. 1364–1386, 2008.

[7] Y. Oshima, K. Kawaguchi, S. Tanaka, K. Ohkawara, Y. Hikihara, K. Ishikawa-Takata, I. Tabata, Classifying Household and Locomotive Activities Using a Triaxial Accelerometer, Gait & Posture, vol. 31, no. 3, pp. 370–374, 2010. Networks (BSN), pp. 24-29, 2010.

[8] J. Wang, R. Chen, X. Sun, M. She, Y. Wu, Recognizing Human Daily Activities from Accelerometer Signal, Procedia Engineering, vol. 15, pp. 1780-1786, 2011.

[9] A. Mitas, M. Rudzki, W. Wieclawek, P. Zarychta, S. Piwowarski, Wearable System for Activity Monitoring of the Elderly. In: E. Pietka, J. Kawa, W. Wieclawek (eds.) Information Technologies in Biomedicine, Advances in Intelligent Systems and Computing, Springer-Verlag, (in press).

[10] S. Borik, B. Babusiak, I. Cap, Device for Accelerometer and Gyroscope Measurements. In: E. Pietka, J. Kawa, W. Wieclawek (eds.) Information Technologies in Biomedicine, Advances in Intelligent Systems and Computing, Springer-Verlag, (in press).

[11] F. Zhou, Y. Wu, N. Fan, Improved accelerometer and magnetometer-based solution to solve quaternion. In: Control, Automation and Systems (ICCAS), 2012 12th International Conference on, IEEE, 2012, pp. 2093-2096.

[12] A. Oppenheim, R. Schafer, Digital Signal Processing. Prentice Hall, 1975.

[13] R. M. Haralick, L. G. Shapiro, Computer and Robot Vision, vol. 1., Addison-Wesley, 1993.